

## States in $^{85}\text{Kr}$ from the $^{84}\text{Kr}(d, p)$ reaction\*

C. P. Browne,<sup>†</sup> D. K. Olsen, J. Chao, and P. J. Riley

Center for Nuclear Studies, The University of Texas, Austin, Texas 78712

(Received 10 December 1973)

30 states in  $^{85}\text{Kr}$  were investigated via the  $^{84}\text{Kr}(d, p)^{85}\text{Kr}$  reaction using 11.0-MeV deuterons. At least 22 of these states have not been previously reported. Angular distributions were measured from 20 to 160° for transitions to 25 of these states, and were fitted with zero-range distorted-wave Born-approximation calculations. Excitation energies,  $l$  values, spectroscopic factors, and the implied values of  $J^\pi$  are given. Comparisons are made with states of other nuclei having both one neutron less and one neutron more than the  $N = 50$  shell closure.

[ NUCLEAR REACTIONS  $^{84}\text{Kr}(d, p)$ ,  $E = 11.0$  MeV; measured  $\sigma(\theta)$ , levels; deduced  $l, S$  with DWBA analysis. ]

### I. INTRODUCTION

As part of a systematic study of the krypton isotopes, we have made measurements on the  $^{84}\text{Kr}(d, p)^{85}\text{Kr}$  reaction leading to 30 states in  $^{85}\text{Kr}$  up to 4.7 MeV of excitation. Only eight of these states (below 2.4 MeV) have been previously observed; five with the  $^{86}\text{Kr}(d, t)^{85}\text{Kr}$  reaction<sup>1</sup> and six with the  $^{86}\text{Kr}(^3\text{He}, \alpha)^{85}\text{Kr}$  reaction.<sup>2</sup> Both these earlier investigations were made with pickup reactions as opposed to the stripping mechanism of our  $(d, p)$  measurements, and hence tended to excite different states. In the present experiment, the target nucleus has two neutron holes in the  $N = 50$  closed shell and  $J^\pi = 0^+$ . The  $(d, p)$  stripping reaction is thus expected to measure rather accurately the degree of emptiness of the nearly full  $2p_{3/2}$ ,  $2p_{1/2}$ , and  $1g_{9/2}$  shells lying below the closed  $N = 50$  shell, and to identify states beginning with  $2d_{5/2}$ ,  $3s_{1/2}$ ,  $1g_{7/2}$ , and  $2d_{3/2}$  lying above the  $N = 50$  shell. A comparison of the present  $^{84}\text{Kr}(d, p)^{85}\text{Kr}$  results with earlier  $(d, p)$  measurements<sup>3</sup> on the  $N = 50$  closed shell nucleus  $^{86}\text{Kr}$  is of interest. In addition to  $^{87}\text{Kr}$ , there are level schemes of other  $N = 51$  nuclei,  $^{89}\text{Sr}$ ,  $^{91}\text{Zr}$ , and  $^{93}\text{Mo}$ , with which comparisons may be made.

Close comparisons should also be possible with the level structure of  $^{87}\text{Sr}$  which also is one neutron short of the closed shell. The  $^{86}\text{Sr}(d, p)^{87}\text{Sr}$  stripping reaction has been studied by Bercaw and Warner<sup>4</sup> at 20.65 MeV, and by Morton *et al.*<sup>5</sup> at 12 MeV. Their results indicate that the three lowest-lying states in  $^{87}\text{Sr}$  arise from  $1g_{9/2}$ ,  $2p_{1/2}$ , and  $2p_{3/2}$  configurations, with the  $2d_{5/2}$ ,  $3s_{1/2}$ , and  $2d_{3/2}$  shells influencing the spectra above 1 MeV of excitation.

### II. EXPERIMENTAL PROCEDURE

Differential cross sections of the  $^{84}\text{Kr}(d, p)^{85}\text{Kr}$  reaction and of deuteron elastic scattering from

$^{84}\text{Kr}$  were measured from 20 to 160° in 5° steps at a bombarding energy of 11.0 MeV. The target gas was contained in a 7.5-cm-diam cylindrical cell whose walls were of 3- $\mu\text{m}$  Mylar foil. Nickel windows of 0.5- $\mu\text{m}$  thickness were used for the beam entrance and exit. The gas pressure was approximately 0.025 atm corresponding to a target thickness of about  $(80/\sin\theta)$   $\mu\text{g}/\text{cm}^2$ . The gas was isotopically enriched to 90.1% of  $^{84}\text{Kr}$ . Four lithium-drifted-silicon detectors, cooled to dry ice temperature, were mounted at 20° intervals on a rotatable place centered on the gas cell. The over-all energy resolution was about 30 keV.

Two different target cells were used. The first employed conventional two-slit collimation for each detector.<sup>6</sup> The second utilized a thin-walled beam tube of 5.0-mm i.d. inside the target cell. A 1.27-cm gap in this tube at the center of the chamber defined the target volume. Consequently, the number of target atoms is approximately the same for all detector angles, which facilitates forward angle measurements.<sup>7</sup> We were gratified to measure the same absolute differential cross sections with both sets of apparatus. Over 60 spectra were analyzed, allowing a good check on the consistency of the measurements.

Eight of the spectra taken at angles from 40 to 160° were used to calculate excitation energies of  $^{85}\text{Kr}$  states. The linear energy calibration for each spectrum was based on the laboratory energies of the  $^{85}\text{Kr}$  g.s., the  $^{87}\text{Kr}$  g.s. (from the 4% of  $^{86}\text{Kr}$  in the target gas), and the elastic deuteron group. The  $^{85}\text{Kr}$  g.s. group and the elastic deuteron group spanned the energy region of interest, whereas the  $^{87}\text{Kr}$  g.s. group was about 1.6 MeV below the  $^{85}\text{Kr}$  g.s. group. To calculate the energies of these groups we used the beam energy obtained from the beam-analyzing magnet and the ground-state  $Q$  values, calculated from mass values<sup>8</sup> of 4.886 MeV for the  $^{84}\text{Kr}(d, p)^{85}\text{Kr}$  reaction and 3.286

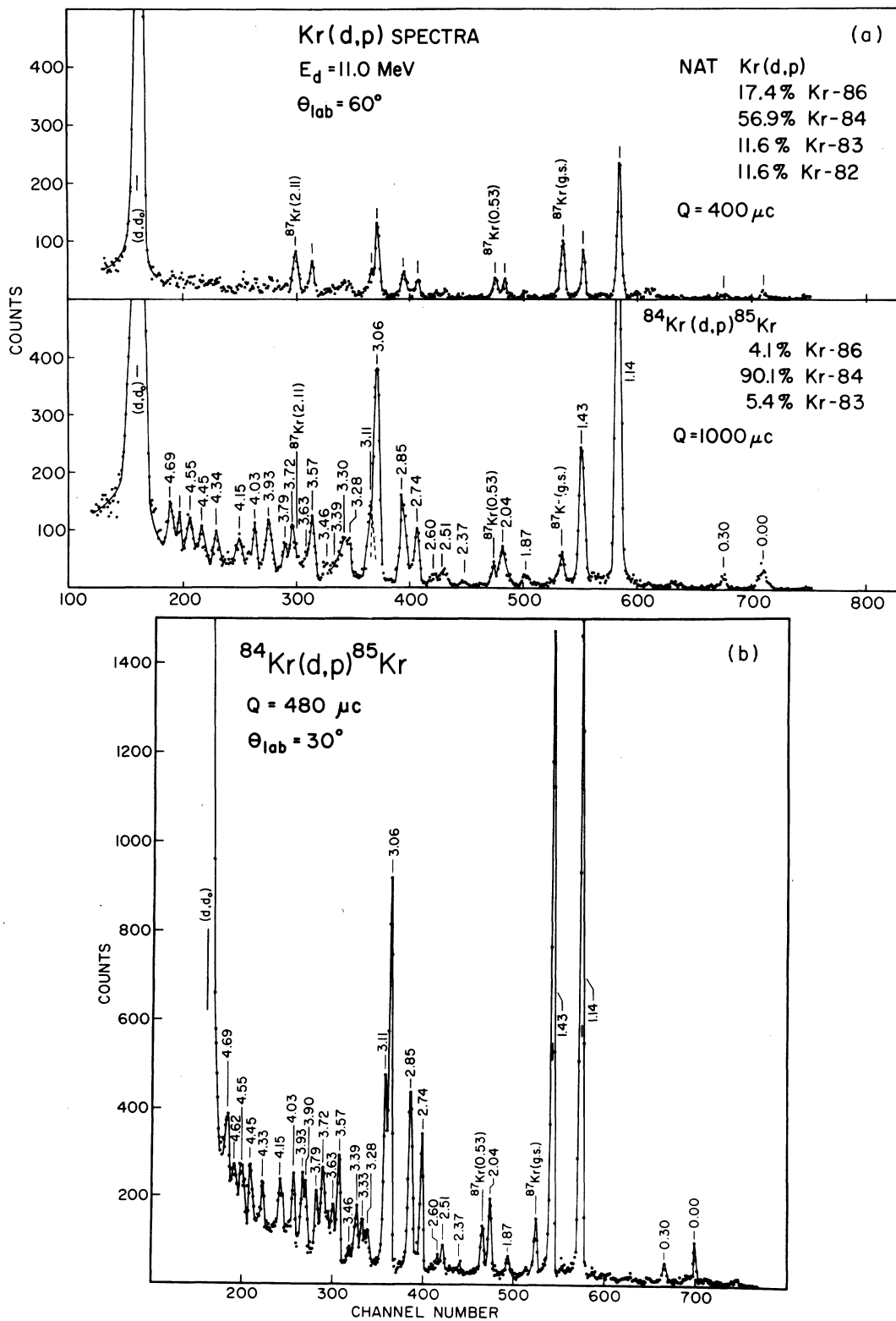


FIG. 1. Spectra measured with cooled lithium-drifted silicon detectors. (a) shows a comparison of natural krypton with enriched krypton used to identify  $^{85}\text{Kr}$  states taken with the two-slit apparatus. (b), showing an improved resolution, was taken with a tube used to define the target volume.

MeV for the  $^{86}\text{Kr}(d, p)^{87}\text{Kr}$  reaction.

### III. ENERGY LEVELS

Figure 1(a) shows typical spectra obtained with the two-slit apparatus<sup>6</sup>; one spectrum with the enriched  $^{84}\text{Kr}$  gas and one spectrum with natural krypton gas. Note the  $^{85}\text{Kr}$  and  $^{87}\text{Kr}$  ground-state groups and the deuteron elastic group, which were used for energy calibration. Somewhat better resolution was achieved when the tube defined the target volume, and in these spectra the 3.06- and 3.11-MeV states were resolved, as shown in Fig. 1(b). We identified the groups corresponding to  $^{85}\text{Kr}$  states by comparing intensities from the enriched and natural krypton targets.

Table I shows the excitation energies of the states found in  $^{85}\text{Kr}$ . The values are the averages

TABLE I. Energy levels of  $^{85}\text{Kr}$ .

Level No.	$E^*$ (MeV) <sup>a</sup> ( $d, p$ )	$E^*$ (MeV) <sup>b</sup> ( $d, t$ )	$E^*$ (MeV) <sup>c</sup> ( $^3\text{He}, \alpha$ )
1	0.00	0.00	0.00
2	0.303 (1.00)	0.305	0.31 1.05
3	1.136	1.12	1.14
4	1.427	1.44	
5	1.868	2.05	1.89
6	2.043	2.20	2.03
7	2.369		2.38
8	2.514		
9	2.598		
10	2.736		
11	2.848		
12	3.055		
13	3.109		
14	3.277		
15	3.326		
16	3.390		
17	3.456		
18	3.565		
19	3.628		
20	3.717		
21	3.787		
22	3.896		
23	3.928		
24	4.027		
25	4.146		
26	4.335		
27	4.450		
28	4.547		
29	4.623		
30	4.692		

<sup>a</sup> Present work.

<sup>b</sup> B. Rosner and E. J. Schneid, Nucl. Phys. **82**, 182 (1966).

<sup>c</sup> C. M. Fou and R. W. Zurmühle, Phys. Rev. **176**, 1339 (1968).

of those from seven or eight spectra and the standard deviations of the mean range from 1 to 6 keV and average 2.7 keV. Three excitation energies in  $^{87}\text{Kr}$  were also measured. These values averaged within 4 keV of those given by Haravu, Hollas, Riley, and Coker.<sup>3</sup> Uncertainties in the  $^{85}\text{Kr}$  excitation energies total perhaps 10 keV.

We also show in Table I excitation energies from previous work. The ( $^3\text{He}, \alpha$ ) measurement of Fou and Zurmühle<sup>2</sup> had about 150-keV resolution and uncertainties of about 50 keV, whereas the ( $d, t$ ) work of Rosner and Schneid<sup>1</sup> was done with 200-keV resolution. There is evidence that the ( $d, t$ ) excitation energies are about 8% too high,<sup>2</sup> so that the 1.12-, 2.05-, and 2.20-MeV states observed in ( $d, t$ ) are probably identical with the 1.05-, 1.89-, and 2.03-MeV levels in ( $^3\text{He}, \alpha$ ). For the 1.136-, 1.868-, and 2.043-MeV states the angular momentum transfer values deduced from our ( $d, p$ ) stripping reaction measurements disagree with those of the ( $^3\text{He}, \alpha$ ) pickup reaction, so that the two reactions may not be populating the same states. There does, however, appear to be a one-to-one correspondence of observed energy levels in the two reactions.

### IV. ANALYSIS OF ANGULAR DISTRIBUTIONS

The optical-model parameters needed to calculate the distorted waves in the entrance and exit channels for the distorted-wave Born-approximation (DWBA) calculations were obtained by fitting  $^{86}\text{Kr}(p, p)$  and  $^{84}\text{Kr}(d, d)$  elastic scattering data. The optical parameters were obtained using

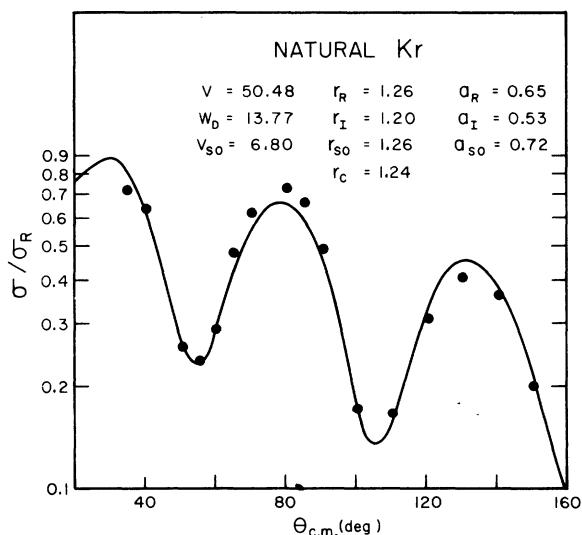


FIG. 2.  $\text{Kr}(p, p)\text{Kr}$  angular distribution data taken at  $E_p = 12.0$  MeV. The solid line is an optical-model fit to the data obtained with the indicated parameters.

a code written by Tamura and Bledsoe<sup>9</sup>; in both cases the usual form for the potential with a surface absorptive term and a real Thomas-type spin-orbit term was used<sup>10</sup>: The optical-model fit to 12-MeV proton scattering data from natural krypton and the resulting optical-model parameters are shown in Fig. 2. Figure 3 shows the deuteron elastic cross sections, the fit, and the optical-model parameters deduced.

Differential cross sections for  $(d, p)$  transitions to 25 of the states in  $^{85}\text{Kr}$ , which were sufficiently populated and resolved, were fitted. A zero-range DWBA code (VENUS) written by Tamura, Coker, and Rybicki,<sup>11</sup> and modified by an approximation for the nonlocality of the optical potential, was used. The bound state neutron wave functions were calculated using the code NEPTUNE.<sup>11</sup> A Woods-Saxon well having essentially the same geometry as the real part of the proton optical potential was chosen for the form-factor calculation. A search for the Woods-Saxon well depth was made to reproduce the experimentally determined separation energy of each level. An energy-dependent proton optical-model real well depth  $V = (54.08 - 0.30E)$  MeV was used for the DWBA fits.

The experimental angular distributions for states of  $^{85}\text{Kr}$  are shown together with the DWBA fits in Figs. 4-7. The agreement between data and the DWBA predictions is reasonably good and we are confident of the  $l$  values deduced. Figure 4 shows that the ground state, 0.30-, 1.14-, and 1.43-MeV states are, respectively, populated by

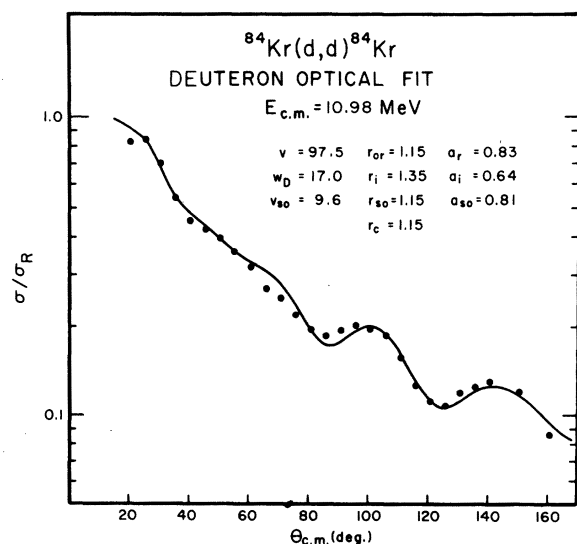


FIG. 3. Angular distribution of deuterons elastically scattered from  $^{84}\text{Kr}$  and the resulting optical-model fit. The optical-model parameters are as shown.

$l=4, 1, 2$ , and 0 transitions. The value  $l=4$  is expected for the  $\frac{9}{2}^+$  g.s. as is  $l=1$  for the known  $\frac{1}{2}^-$  first excited state. The 1.14-MeV state is assigned to be  $\frac{5}{2}^+$  on the basis of conventional shell-model ordering of states and the 1.43-MeV state is clearly  $\frac{1}{2}^+$ .

Figure 5 shows four additional  $l=2$  transitions. Two curves are shown for the 2.04-MeV state, one for  $d_{3/2}$  and one for  $d_{5/2}$ . Clearly from the data one cannot choose between them. Figures 6 and 7 show the data and DWBA predictions for the remaining angular distributions that could be fitted.

Table II gives a summary of the results of the calculations. For  $l=0$  transitions the  $J^\pi$  values can of course only be  $\frac{1}{2}^+$ . Where a single  $J$  value

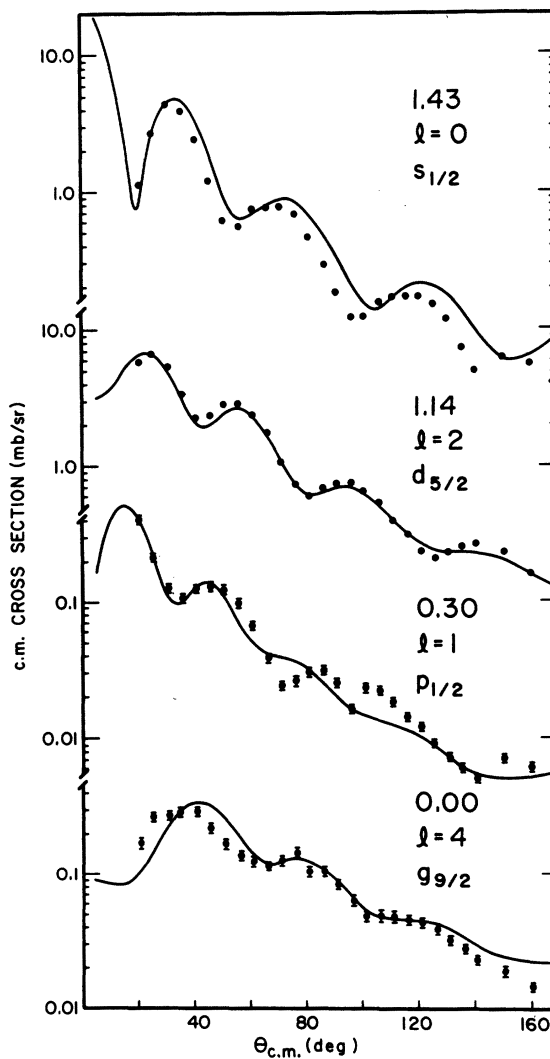


FIG. 4. Angular distributions of the  $^{84}\text{Kr}(d, p)^{85}\text{Kr}$  reaction leading to the ground state and three low-lying excited states. The curves are DWBA fits. Excitation energies, deduced  $l$  values, and inferred  $l_j$  values are as shown.

is indicated for nonzero  $l$  values we have assumed the usual shell-model ordering of states. The last column of the table gives the spectroscopic factor  $S_J$  defined as

$$S_J = \sigma_{\text{expt}} / [(2J+1)\sigma_{\text{DWBA}}].$$

Two values are shown for  $S_J$  when there are two possible  $J$  values.

Figure 8 shows an energy-level diagram of the states for which we have deduced  $l$  values and also shows states of  $^{87}\text{Sr}$ , a nucleus with the same number of neutrons as  $^{85}\text{Kr}$ . The length of the lines is proportional to the spectroscopic factors. The  $^{87}\text{Sr}$  parameters are a composite of the 12-MeV ( $d, p$ ) work of Morton *et al.*<sup>5</sup> and the 20.6-MeV ( $d, p$ ) work of Bercaw and Warner.<sup>4</sup> Correspondence

of the g.s.,  $\frac{1}{2}^-$ ,  $\frac{5}{2}^+$ , and first  $\frac{1}{2}^+$  states is seen. One or two more  $l=2$  states may also correspond with  $^{87}\text{Sr}$  states including the 3.06-MeV,  $\frac{3}{2}^+$  state.

The ground-state spectroscopic factor of 0.194 would indicate that the  $g_{9/2}$  orbit in  $^{84}\text{Kr}$  is about 80% filled. The  $^{85}\text{Kr}$  0.30-MeV  $\frac{1}{2}^-$  state with a spectroscopic factor of 0.077 is indicative of a small  $2p_{1/2}$  admixture in the target configuration. The situation is similar in  $^{87}\text{Sr}$ . The  $\frac{5}{2}^+$ ,  $\frac{1}{2}^+$ , and  $\frac{3}{2}^+$  states indicate the filling of the vacant  $2d_{5/2}$ ,  $3s_{1/2}$ , and  $2d_{3/2}$  shells. The present experiment, in slight disagreement with the  $^{86}\text{Sr}(d, p)$  work, does not indicate a second  $l=1$  transition—if it is present in  $^{85}\text{Kr}$ , it is very weak. Thus, apparently the  $1f_{5/2}$  and the  $2p_{3/2}$  subshells are virtually full in  $^{84}\text{Kr}$ .

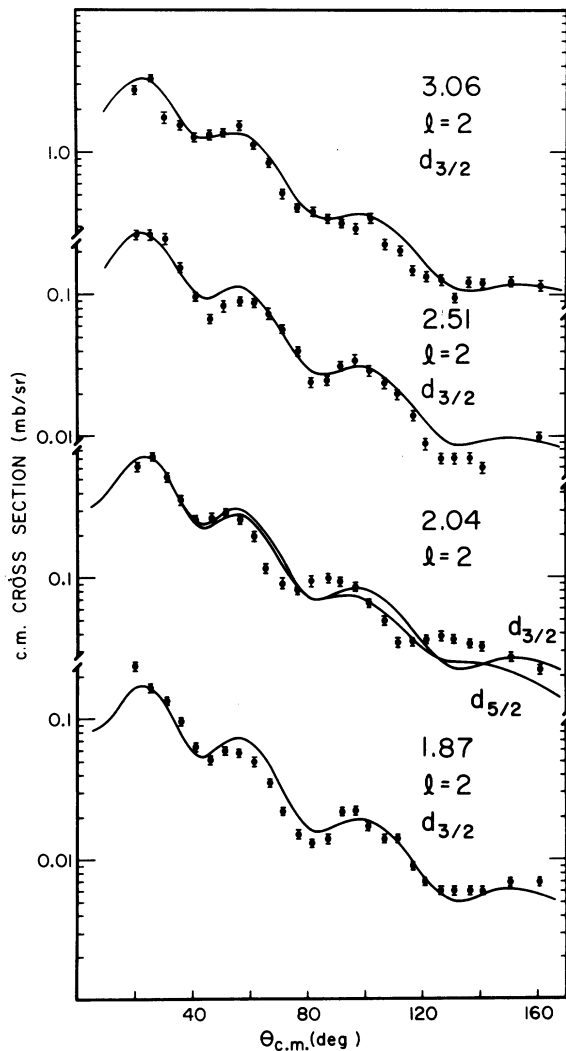


FIG. 5.  $^{84}\text{Kr}(d, p)^{85}\text{Kr}$  angular distribution data and the resulting DWBA fits for four low-lying  $l=2$  states. The  $l_j$  values used to obtain the fits are indicated on the figure.

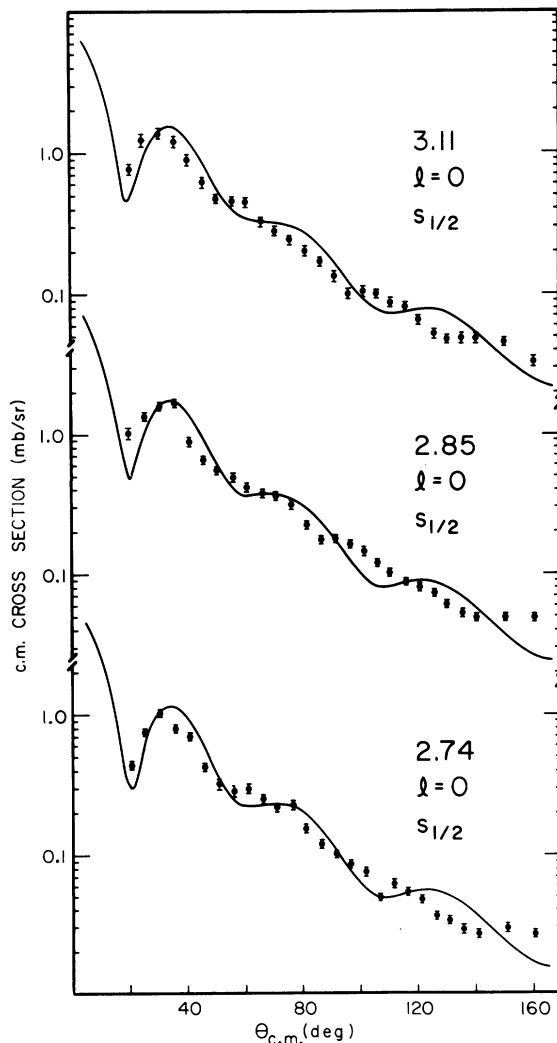


FIG. 6.  $^{84}\text{Kr}(d, p)^{85}\text{Kr}$  angular distribution data and the resulting DWBA fits for three  $l=0$  states.

We find only one strong  $l=2$  state below the first  $l=0$  state, whereas in  $^{87}\text{Se}$  there are two. The strong 3.05-MeV state probably marks the onset of the  $2d_{3/2}$  subshell; however, the weak  $l=2$  states could be either  $\frac{5}{2}^+$  or  $\frac{3}{2}^+$ . At 3.39 MeV

excitation we find a second  $l=4$  state, indicative of the  $1g_{7/2}$  subshell. The  $1h_{11/2}$  subshell may lie above the excitation energy range of this experiment.

Figure 9 compares the levels of  $^{85}\text{Kr}$  with those

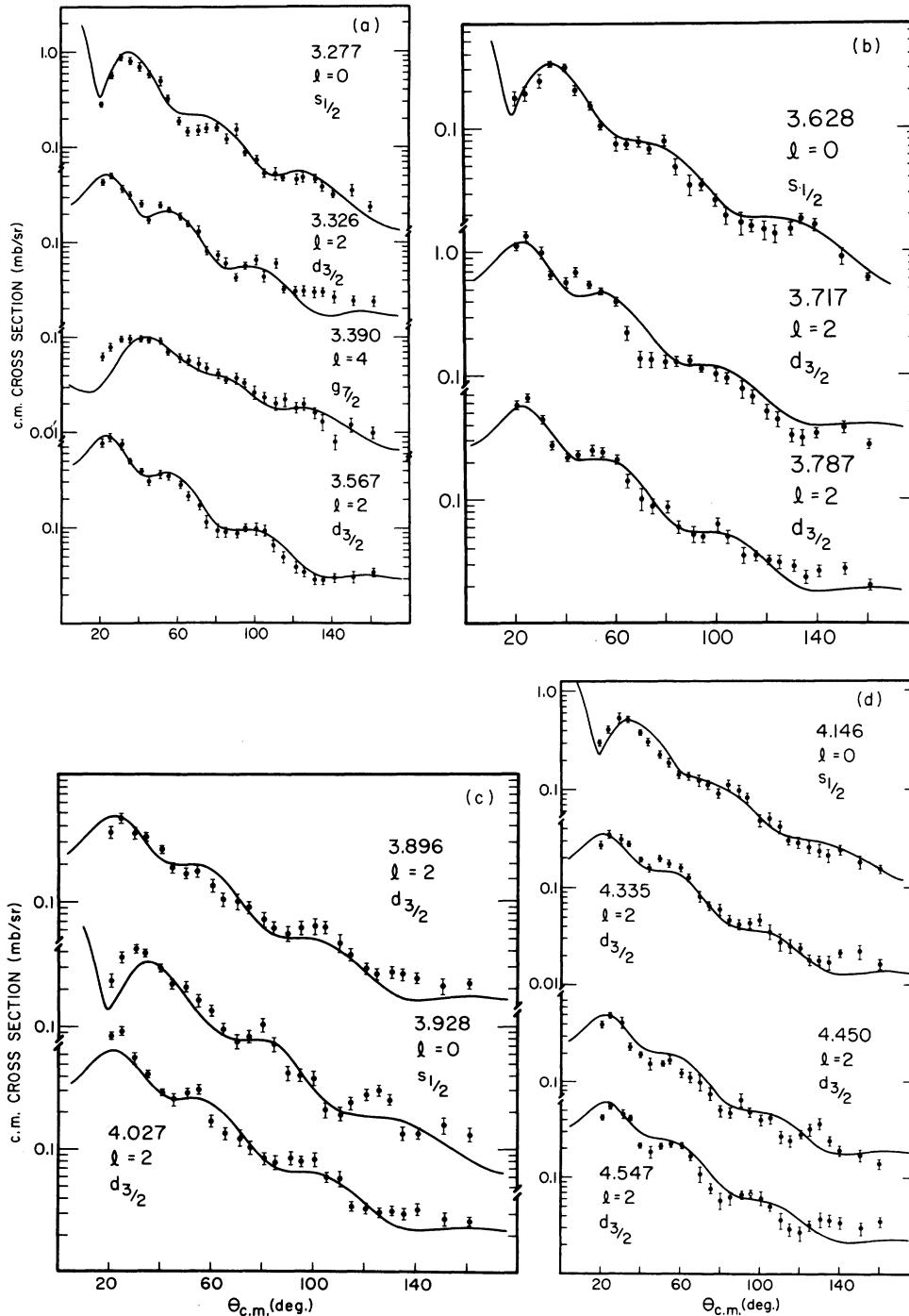


FIG. 7.  $^{84}\text{Kr}(d,p)^{85}\text{Kr}$  angular distribution data and the resulting DWBA fits for 14 states with excitation energies between 3.277 and 4.547 MeV. The  $l_j$  values used to obtain the respective fits are indicated on the figures.

of nuclei having two additional neutrons ( $N = 51$ ). The 1.14-MeV,  $\frac{5}{2}^+$  state of  $^{85}\text{Kr}$  is aligned with the  $\frac{5}{2}^+$  g.s. of  $^{87}\text{Kr}$ . The rest of the figure is taken from Haravu *et al.*<sup>3</sup> The  $\frac{1}{2}^+$  state and the  $l=2$  state at 3.05 MeV in  $^{85}\text{Kr}$  seems to be consistent with similar states arising from the  $3s_{1/2}$  and  $2d_{3/2}$  subshells, respectively, in the other nuclei. The 2.51-MeV state in  $^{85}\text{Kr}$  may have a similar configuration to the second  $l=2$  states in the other nuclei.

#### SUMMARY AND DISCUSSION

30 states of  $^{85}\text{Kr}$  with excitation energy up to 4.7 MeV have been observed via the reaction  $^{84}\text{Kr}(d, p)^{85}\text{Kr}$ . The orbital angular momenta transfer values have been obtained for 25 of these states through DWBA calculations. 8  $l=0$ , 1  $l=1$ , 14  $l=2$ , and 2  $l=4$  transfer values have been assigned. The spin assignments for the two  $l=4$  states (g.s. and 3.39-MeV state), and for the  $l=1$  state at 0.30 MeV, have been made

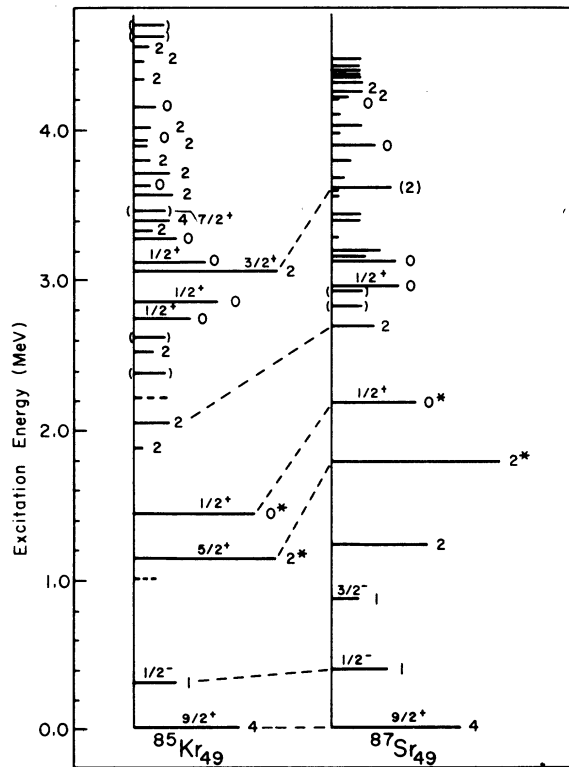


FIG. 8. A comparison of the  $^{85}\text{Kr}_{49}$  energy levels with the  $^{87}\text{Sr}_{49}$  energy levels. The lengths of the lines are proportional to the spectroscopic factors. An asterisk indicates that the spectroscopic factor is twice that shown. The numbers at the ends of the lines are the measured  $l$  values. The more certain  $J^\pi$  values are indicated.

on the basis of the conventional shell-model ordering of states. The observed weak  $l=1$  state at 0.30 MeV is indicative of some configuration mixing in the ground state of  $^{84}\text{Kr}$ . The only definitive spin assignment for the  $l=2$  states is that of  $\frac{5}{2}^+$  for the 1.136-MeV state, which, as the first strongly excited state, is clearly indicative of the filling of the first  $2d_{3/2}$  subshell above  $N = 50$ . Similarly, the strong  $l=2$  state at 3.055 MeV probably indicates the beginning of the  $2d_{3/2}$  subshell; however, the assignment of  $\frac{3}{2}^+$  to this state can only be tentative.

TABLE II. Summary of the DWBA analysis of the states of  $^{85}\text{Kr}$  via the reaction  $^{84}\text{Kr}(d, p)^{85}\text{Kr}$ .

Level No.	$E^*$ (MeV)	$l$	$J^\pi$	$S_J$
1	0.000	4	$\frac{9}{2}^+$	0.194
2	0.303	1	$\frac{1}{2}^-$	0.077
3	1.136	2	$(\frac{5}{2})^+$	0.545
4	1.427	0	$\frac{1}{2}^+$	0.453
5	1.868	2	$(\frac{5}{2}, \frac{3}{2})^+$	0.013, 0.018
6	2.043	2	$(\frac{5}{2}, \frac{3}{2})^+$	0.049, 0.075
8	2.514	2	$(\frac{5}{2}, \frac{3}{2})^+$	0.017, 0.025
10	2.736	0	$\frac{1}{2}^+$	0.099
11	2.848	0	$\frac{1}{2}^+$	0.157
12	3.055	2	$(\frac{5}{2}, \frac{3}{2})^+$	0.179, 0.274
13	3.109	0	$\frac{1}{2}^+$	0.134
14	3.277	0	$\frac{1}{2}^+$	0.087
15	3.326	2	$(\frac{5}{2}, \frac{3}{2})^+$	0.027, 0.041
16	3.390	4	$(\frac{7}{2})^+$	0.062
17	3.456	...	...	...
18	3.565	2	$(\frac{5}{2}, \frac{3}{2})^+$	0.044, 0.069
19	3.628	0	$\frac{1}{2}^+$	0.030
20	3.717	2	$(\frac{5}{2}, \frac{3}{2})^+$	0.058, 0.083
21	3.787	2	$(\frac{5}{2}, \frac{3}{2})^+$	0.026, 0.039
22	3.896	2	$(\frac{5}{2}, \frac{3}{2})^+$	0.022, 0.033
23	3.928	0	$\frac{1}{2}^+$	0.027
24	4.027	2	$(\frac{5}{2}, \frac{3}{2})^+$	0.030, 0.042
25	4.146	0	$\frac{1}{2}^+$	0.043
26	4.335	2	$(\frac{5}{2}, \frac{3}{2})^+$	0.015, 0.023
27	4.450	2	$(\frac{5}{2}, \frac{3}{2})^+$	0.021, 0.031
28	4.547	2	$(\frac{5}{2}, \frac{3}{2})^+$	0.024, 0.037
29	4.623	...	...	...
30	4.692	...	...	...

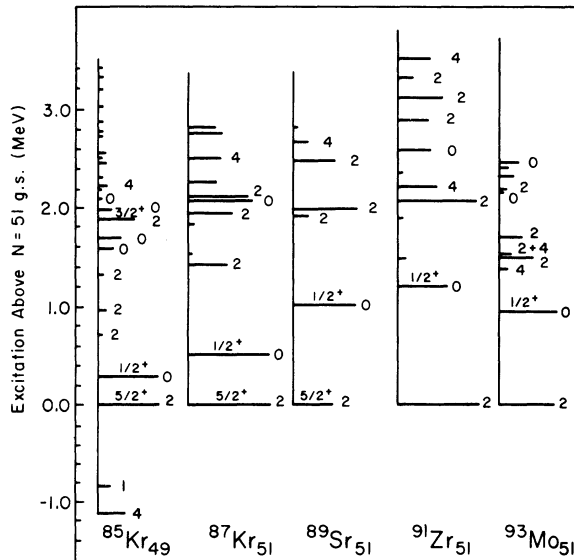


FIG. 9. A comparison of the  $^{85}\text{Kr}_{49}$  energy levels with those of four nuclei having two additional neutrons ( $N=51$ ). The ground states of these nuclei are used for the zero of the excitation energy scale. The 1.14-MeV  $l=2$  state of  $^{85}\text{Kr}$  is assumed to correspond to the  $5/2^+$  orbit above the  $N=50$  closed shell and thus to correspond to the ground states of the  $N=51$  nuclei. It is so aligned in the figure. The lengths of the horizontal lines are proportional to the spectroscopic factors.

The ground-state spectroscopic factor of 0.194 indicates that the  $1g_{9/2}$  orbit is about 80% full in  $^{84}\text{Kr}$ . The sum of the spectroscopic factors for the  $1/2^+$  states is 1.03 which, within experimental error, exhausts the sum rule for  $3s_{1/2}$  transitions. If we somewhat arbitrarily assign the four  $l=2$

transitions to states below 3.055 MeV of excitation to be  $2d_{5/2}$  transfers, and the remaining  $l=2$  transitions to be  $2d_{3/2}$  transfers, then the sum of the  $2d_{5/2}$  and  $2d_{3/2}$  spectroscopic factors are 0.62 and 0.67, respectively. Probably some of the  $l=2$  states above 3.055 MeV of excitation are  $5/2^+$  rather than  $3/2^+$ . In any case, the 30 transitions considered here do not exhaust the  $2d_{3/2}$  and  $2d_{5/2}$  strength.

Another important set of numbers from this work are the spectroscopic-factor-weighted energy centroids  $\bar{E}_J$ . These centroids are defined by the equation

$$\bar{E}_J = \frac{\sum_i E_i^* S_J^i}{\sum_i S_J^i}, \quad (2)$$

where  $i$  counts the states for a given  $J$ . For the  $3s_{1/2}$  states we obtain  $\bar{E}_{1/2}$  to be 2.39 MeV. Again, assuming that the  $l=2$  states above and including the 3.055-MeV state are  $2d_{3/2}$  and the four lowest-energy  $l=2$  states are  $2d_{5/2}$ , we obtain  $\bar{E}_{5/2}$  to be 1.26 MeV and  $\bar{E}_{3/2}$  to be 3.54 MeV.

Over all, the states of  $^{85}\text{Kr}$  indicate a rather close correspondence with those of  $^{87}\text{Sr}$ , except that the single-particle orbitals appear to lie at a somewhat lower excitation energy in  $^{85}\text{Kr}$ . The  $l=2, 0$ , and 4 states in  $^{85}\text{Kr}$  above the  $N=50$  shell also show a close correspondence with those of the 51-neutron nuclei  $^{87}\text{Kr}$ ,  $^{89}\text{Sr}$ ,  $^{91}\text{Zr}$ , and  $^{93}\text{Mo}$ , although greater fractionation of the single-particle states is evident for  $^{85}\text{Kr}$ . Polarization measurements would allow us to establish uniquely many  $J$  assignments in  $^{85}\text{Kr}$ . High-resolution spectrograph measurements would help to confirm the level structure, and resolve possible doublet states. Such work is planned at Notre Dame.

\*Work supported in part by the U. S. Atomic Energy Commission.

†Permanent address: Department of Physics, University of Notre Dame, Notre Dame, Indiana 46556.

<sup>1</sup>B. Rosner and E. J. Schneid, Nucl. Phys. **82**, 182 (1966).

<sup>2</sup>C. M. Fou and R. W. Zurmühle, Phys. Rev. **176**, 1339 (1968).

<sup>3</sup>K. Haravu, C. L. Hollas, P. J. Riley, and W. R. Coker, Phys. Rev. C **1**, 938 (1970).

<sup>4</sup>R. W. Bercaw and R. E. Warner, Phys. Rev. C **2**, 297 (1970).

<sup>5</sup>J. M. Morton, W. G. Davis, W. McLatchie, W. Carcey, and J. E. Kitching, Nucl. Phys. **A161**, 228 (1971).

<sup>6</sup>L. A. Silverstein, Nucl. Instrum. Methods **4**, 53 (1959).

<sup>7</sup>J. D. Garret, Ph. D. thesis, University of Pennsylvania, 1970 (unpublished).

<sup>8</sup>N. B. Gove and A. H. Wapstra, Nucl. Data **A11**, 127 (1972).

<sup>9</sup>T. Tamura and H. Bledsoe, private communication.

<sup>10</sup>S. Sen, C. L. Hollas, C. W. Bjork, and P. J. Riley, Phys. Rev. C **5**, 1278 (1972).

<sup>11</sup>T. Tamura, W. R. Coker, and F. Rybicki, Comput. Phys. Commun. **2**, 94 (1971).